ENHANCEMENT OF PV PANEL'S POWER USING CLOSED BACK SIDE COOLING SYSTEM AND NUMERICAL SIMULATION

Stefan N. DJORDJEVIC[a], Marko S. KRSTIC[a], Lana S. PANTIC[a], Ivana S. RADONJIC[a], Marko V. MANCIC[b], Veljko S. BEGOVIC[b], Sasa R. GOCIC[a], Branka G. RADOVANOVIC[b]

[a] Faculty of Sciences and Mathematics, Department of Physics, University of Niš,

[b] Faculty of Mechanical Engineering, University of Niš

[*] Corresponding author; E-mail: stefan.djordjevic1@pmf.edu.rs

The efficiency of photovoltaic (PV) panels is significantly influenced by the temperature of the cells, as higher temperatures reduce electrical power output, degrade performance, and shorten the panel's lifespan. This study investigates the effectiveness of a closed-loop cooling system applied to the backside of a PV panel to enhance its output characteristics. The cooling system circulated approximately 20 liters of water at a constant flow rate of 70 L/h. The results demonstrated a substantial 41.75% increase in power output, with the maximum efficiency achieved at peak cooling. Using real weather data recorded during the experiment, the temperature distribution across the panel layers was modeled using the ANSYS FLUENT 2023 R1 software package. The simulation and experimental results showed a maximum temperature difference of 1.6 °C between the measured and simulated values. The cooled panel maintained an average temperature of 26.65 °C, with a minimum of 16.7 °C, compared to an uncooled panel's higher temperatures. The system effectively reduced the temperature of the front side of the panel by up to 23.1 °C, enhancing the overall energy output. These findings confirm that cooling PV panels from the back is an efficient method to reduce temperature and increase panel efficiency. Detailed simulations and analyses enable insight into PVT system performance and forecasting of production under various climatic conditions.

Key words*: PV panel, back side cooling, power enhancement, electrical efficiency, ANSYS simulation.*

1. Introduction

Rapid global population growth nowadays has created enormous demand for resources such as electrical energy, leading to a dramatic increase in fossil fuel consumption. The use of fossil fuels in power plants, including coal, and natural gas, requires careful restriction due to significant carbon dioxide emissions into the atmosphere, which negatively impact the environment. Transitioning to alternative energy sources such as wind, solar, geothermal and biomass energy can significantly contribute to reducing environmental load. Solar energy stands out as a clean and inexhaustible energy source. It can be utilized for heating water in solar thermal system and for generating electricity through photovoltaic (PV) solar cells [1].

The efficiency of the PV systems ranges between 10% and 20%, while the thermal system has an efficiency of between 40% and 60% [2]. The efficiency of the PV panels is especially influenced by the temperature of the PV cells and the intensity of sunlight [3]. Higher temperatures of PV cells reduce electrical power output, degrade performance, and impact the lifetime of PV panels [4]. Thus, it is essential to reduce the temperature of PV cells to enhance their performance. Integrating PV and solar thermal technologies into a single system creates a photovoltaic thermal (PVT) system. The PVT system typically consists of a heat exchanger made of tubes or channels positioned on the back side of the PV panels. This heat exchanger utilizes the heat generated during their operation to heat a fluid, enabling simultaneous production of electricity and thermal energy. If the fluid circulates inside a heat exchanger and takes the heat from the PV panel, it results in increasing efficiency. Active cooling technology based on PVT collectors enables higher efficiency of PV solar cells by converting solar radiation directly into electricity while also generating heat.

Numerous studies have been conducted to find a suitable fluid and method for efficient heat transfer from PV modules and increase the efficiency of PVT systems. Moharram *et al.* [5] were studying methods on how to increase the efficiency of PV panels. They developed a water spraying cooling system, incorporating mathematical models to determine the optimal timing and duration of cooling cycles. The cooling of the panels is performed by starting the system for 5 minutes each time, with a cooling rate of 2 $^{\circ}$C/min which leads to a PV panel temperature reduction by 10 °C. Al-Jamea *et al.* [6] compares immersion and spraying water-cooling systems for enhancing PV power and efficiency. Spraying water on the PV surface resulted in a more significant enhancement of the PV panel's electrical performance parameters compared to submerging the panel. Using the spraying method lowered PV temperature to 34.3 °C and increased power output by 59% compared to non-cooled panel. Kumar *et al.* [7] developed an analytical model to analyze the electrical and thermal performances of a PV panel with top water-cooling under Chennai, India, weather conditions. The results indicate that water-cooling on the panel reduces daily average PV panel temperature from 56.67°C to 39.44 °C, enhancing daily electrical efficiency from 12.74% to 14.29%.

Except water, various fluids such as ethanol, ethylene glycol, and acetone have been tested to achieve high efficiency of PVT systems [8, 9]. Using nanofluids as a working fluid in the PVT system is recognized as an effective method to improve its efficiency. Elmir *et al.* [10] conducted one of the initial studies on using nanofluid as a cooling medium in PVT systems. Their numerical investigation was focused on cooling a photovoltaic unit using Al_2O_3–water nanofluid and assessed its impact on heat transfer enhancement within the PVT system. They noted substantial improvements in heat transfer compared to using pure water. Menon *et al.* [11] investigated the performance of an unglazed PVT system incorporating a serpentine coil sheet-and-tube thermal absorber. They analyzed electrical and thermal efficiency using water and copper oxide nanofluid as working fluids. The maximum panel temperature reductions of 15 °C and 23.7 °C were obtained for water and nanofluid cooling, respectively. The water-cooling method enhanced the average electrical efficiency by 12.32% compared to an uncooled PVT system, while the nanofluid cooling further improved it by 35.67%. Rejeb et al. [12] explored the impact of aluminum and copper nanoparticles on the performance of PVT systems using different base fluids, such as water and ethylene glycol. In recent days, the combination of nanofluids and Phase Change Materials (PCMs) has been increasingly used as an advanced cooling technique to enhance the thermal management of PV panels, improving their efficiency and lifespan. PCMs absorb excess heat through latent heat during phase change,

maintaining optimal module temperature and reducing thermal stress. Combining PCMs and nanofluids in hybrid cooling systems can further optimize thermal regulation, resulting in significant improvements in PV module efficiency, especially under high solar radiation conditions. The results indicated that water outperforms ethylene glycol in enhancing the overall system performance.

Detailed simulations and analyses enable the evaluation of performance and improvement of the efficiency of the PVT system under various external conditions. The use of software such as ANSYS or Computational Fluid Dynamics (CFD) allows a comprehensive assessment of fluid flow, heat transfer dynamics, and overall system performance, providing insights into optimizing the design and operational parameters of PVT collectors. Selmi *et al.* [13] utilized CFD software to simulate and analyze flat plate solar energy collector with water flow. Their numerical analysis was concentrated on examining heat transfer mechanisms involving convection and radiation. To validate the results obtained from the CFD simulation model, an experimental model was built. The outlet temperature of water which is obtained by simulation is compared with experimental results and there is a good compliance. Attia *et al.* [14] conducted detailed numerical modeling and comparative analysis on a PVT system with two different cooling channel structures. The first structure represents a standard PVT collector, while the second introduces an innovative design featuring cooling channels divided into three equal sections of zigzag-plated tubes. Each section employs a double-pass configuration with staggered inlet/outlet placements. The results indicate that this modified configuration significantly improved electrical efficiency and demonstrated enhancements of 4% for the water-cooled PVT system. Khelifa *et al.* [15] conducted a detailed numerical analysis on PVT system enhanced with natural porous flax fibers for improved thermal performance. A novel cooling channel integrates these fibers doped in water to enhance photovoltaic panel cooling. Using ANSYS software and the Darcy-Brinkman-Forchheimer porous model, simulations compare this system against PVT system using pure water and air as coolants. Optimal design parameters include 50 mm thickness of flax fibers and a water flowrate of 0.907 m/s, achieving a 173.46% increase in Nusselt number compared to pure water. Thermal efficiencies reach 69.58%, 50.02%, and 34.60% for water with flax fibers, pure water, and air cooling, respectively. He *et al.* [16] conducted a theoretical and experimental investigation of a PVT system integrated into a thermoelectric cooling and heating unit. They observed electrical and thermal efficiencies of 16.7% and 23.5%, respectively. The solar radiation in their experiments varied between 200 and 700 W/m². Attia *et al.* [17] explored the bi-fluid photovoltaic thermal (BFPVT) system, utilizing dual coolants to enhance electrical and thermal performance. The research focuses on a 3-D numerical investigation of BFPVT systems cooled by natural air and water/TiO_2 nanofluid through different channel structures. Parametric analysis reveals that higher TiO_2 nanoparticle concentrations improve cooling rates and thermal efficiency. The optimal configuration includes 1.0% TiO_2 nanoparticles and eight longitudinal fins, achieving peak thermal efficiencies of 78.6% and 70.8% for finned and non-finned setups, respectively. Bahaidarah *et al.* [18] focuses on enhancing the performance of PV modules through a hybrid water-cooled system. A numerical model using Engineering Equation Solver (EES) software is developed to simulate electrical and thermal parameters, while experimental validation in Dhahran, Saudi Arabia confirms its accuracy. By integrating a heat exchanger (cooling panel) at the rear surface, the panel's temperature is reduced by approximately 20%, resulting in a 9% increase in PV panel efficiency with active water cooling. Muslim *et al.* [19] investigated the impact of water-cooling on PV panels for enhanced electrical efficiency. A water-cooling chamber attached to the back of PV panels was tested with

different panel orientations (60°, 30°, 0°) and reverse water flow directions. Results show significant improvements in thermal efficiency (up to 80%) and electrical efficiency (up to 17%) with cooling, particularly at higher flow rates (4 l/min), reducing PV temperature and increasing electric parameters across all tested configurations compared to uncooled panels. Fakouriyan *et al.* [20] introduces a novel cooling system for PV panels aimed at enhancing electrical efficiency and providing heated water. The system integrates a single mono-crystalline PV panel with a cooling water system to maintain uniform surface temperatures and a solar water heater to meet domestic hot water needs. Experimental results conducted in Tehran, Iran, demonstrate significant improvements in electrical (12.3%), thermal (49.4%), and overall energy efficiencies (61.7%) compared to conventional systems. Mohamed *et al.* [21] worked on the rise of PV panel efficiency proposing an active closed-loop cooling system. Two water glazing chambers made from acrylic glass are implemented on the front and rear surfaces of the PV panel to cool the cells and filter sunlight. Results indicate a 50.06% reduction in PV cell temperature, resulting increase of 14.2% in electrical efficiency of the PV panel with the cooling system implemented.

The aim of the experiment presented in this paper was to determine the changes in output power of the PV panel, utilizing a design based on a PVT system, but focusing only on the electrical characteristics rather than the thermal properties. Considering experiments from [10-21], we constructed a closed-loop system for active cooling of PV panels. The PV panel was cooled from the back using a closed system, where approximately 20 liters of pure water circulated at a constant mass flow rate of 70 l/h. Water first flowed behind the panel, then passed through an aluminum heat exchanger to reduce its temperature. After being cooled, the water was collected in a tank and pumped back to the back of the panel to continue the cooling process. Continuous measurements of the output power of both the reference and cooled PV panels were conducted before, during, and after the cooling process. The cooling duration was three hours, performed during the time of day with the highest solar radiation intensity. Simulations were performed in parallel using the commercial software package ANSIS FLUENT 2023 R1, to analyze and validate the temperature of the panel in different weather conditions. The simulation models the temperature distribution across the panel layers, with particular emphasis on the temperature distribution on the front side of the PV panel (specifically, the front glass), as thermal imaging during the experiment captured the front surface of the panel. This approach enables a detailed comparison between the simulated and experimental temperature profiles for validation purposes. Real weather conditions recorded during the experiment were used as boundary conditions in the simulation.

2. Experimental setup

The experiment was performed on Jun 4th, from 10:15 a.m. to 1:29 p.m., at the Faculty of Sciences and Mathematics (FSM) building in Niš, Serbia (Latitude: 43.3097° and Longitude: 21.9231°). The experimental setup consists of two 100 Wp, monocrystalline silicon, photovoltaic panels (LUXOR, LX-100M/125-36). The open-circuit voltage, V_{oc}, is 21.6 V, and the short-circuit current, I_{sc}, is 5.87 A. One was used as referent and the second was equipped with a channel on the back side of the panel, which was used for cooling, Fig. 1 (left). The dimensions of the channel were $1194 \times 542 \times 35$ mm and in a closed system circulated about 20 l of pure water with a constant flow of 70 l/h. The area where the junction box is located is uncooled. The panels were fixed under a specific tilt angle of 32° (to obtain the highest electricity output during the year) and mounted on the

roof of the FSM building. The commercial 100 Wp panel consists of 36 monocrystalline solar cells with a dimension of 125 × 125 mm. A schematic diagram of active cooled PV panel based on PVT collectors was shown on picture Fig. 1 (right).

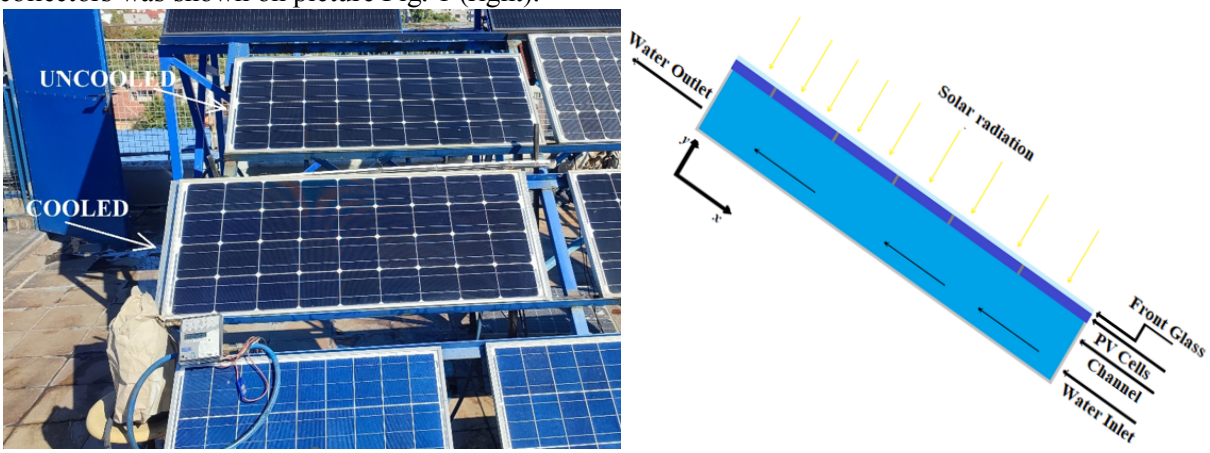

Fig. 1. Experimental setup of the PVT system (left), and schematic diagram of cooled PV panel (right).

The main parts of the test system and the equipment used in the experiment are the custom-made channel, installed on the back side of the panel, a water tank, a circulation pump (power of 5 W), aluminum cooler, Kamstrup MULTICAL 401 device, pyranometer, PV-KLA device, meteorological station and corresponding connections for bringing water into the closed circuit of the system. A schematic diagram of the cooled PV panel is presented in Fig. 2.

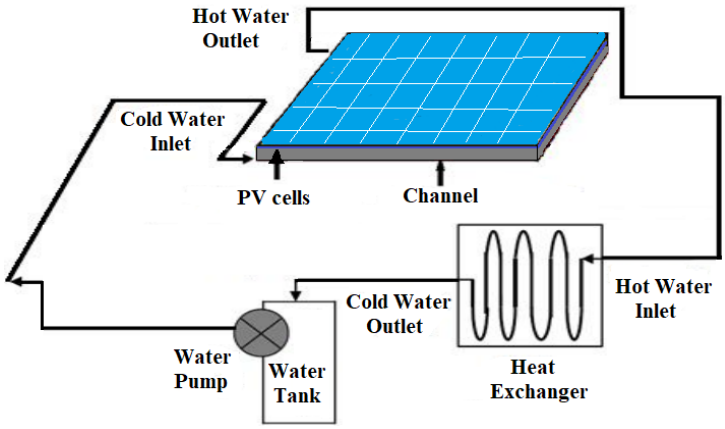

Fig. 2. A scheme of a system for PV panel cooling.

The Kamstrup MULTICAL 401 device is used to measure the temperature of the fluid at the inlet and outlet of the channel, and for measuring the flow rate. The uncertainty in temperature measurement is ± 0.3 °C, while he uncertainty in flow rate measurements is 2%. A FLIR C5 thermal camera was used to monitor the temperature change of the PV panel during the experiment. The accuracy of thermal camera is ±3 °C within the measurement range from 0 °C to 100 °C. The power-voltage characteristics, P-V, and current-voltage characteristics, I-V, of the PV panel were measured with a PV-KLA device, every 2 minutes (log data), the basic accuracy is 0.1% from full scale. The total incident radiation was measured using a PV-KLA device sensor specially made for these purposes, which was placed in parallel to the photovoltaic surface and a Kipp & Zonen pyranometer, as a control. The uncertainty for measuring solar radiation intensity is less than ±1.5% for values less

than 1000 W/m^2. Ambient temperature and wind speed were measured using the DAVIS Vantage PRO meteorological station. The uncertainty in measuring ambient temperature is 0.5 °C, and in measuring wind speed is 1m/sor ± 5%. During the experiment, the working fluid had a constant mass flow at the inlet tube of cooling channel.

2.1. Numerical simulations setup

In parallel, simulations were conducted using the commercial CFD software ANSYS Fluent 2023 R1. This software employs the finite volume method to discretize the computational domain into a finite number of non-overlapping control volumes, transforming the governing partial differential equations (including the Navier-Stokes equations) into a system of algebraic equations that can be solved numerically. This approach enables accurate modeling and analysis of fluid flow and heat transfer phenomena, which are particularly relevant in applications such as solar panel cooling [22].

A three-dimensional model of a PVT collector with an active cooling system was developed in SolidWorks CAD software, Fig. 3. The design incorporated a rectangular water reservoir with inlet and outlet openings located on its underside.

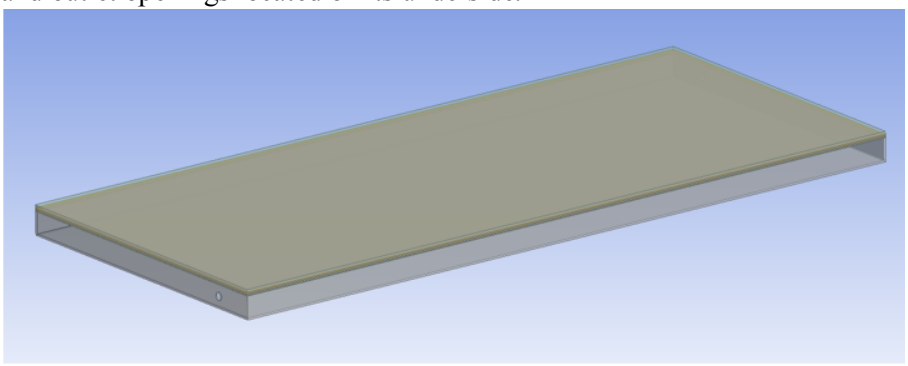

Fig. 3. Geometry model of a PVT collector with an active cooling system

To accurately simulate the thermal performance of the PVT collector, the thermo-physical properties of all materials in the top layer were first specified. For each material (e.g., glass, Tedlar, EVA Superior), density, specific heat capacity and thermal conductivity were defined based on literature data and manufacturer specifications.

The following boundary conditions were defined: the water inlet and outlet temperatures from the reservoir, recorded during the experiment, were set as temperature boundary conditions. The water flow velocity through the reservoir was calculated from the measured flow rate and the cross-sectional area of the inlet pipe. A heat flux was applied to the external, sun-exposed surface of the collector, determined from the solar radiation intensity measurements and the optical characteristics of the collector.

The computational mesh was created using Fluent Meshing and the Watertight Geometry workflow. The presence of five extremely thin layers within the solar panel structure, with the thinnest layer measuring 0.3 mm, posed a significant challenge for meshing. To ensure mesh quality, orthogonal quality was prioritized as a key metric for accurate CFD simulations. An unstructured polyhedral mesh consisting of 4,203.105 elements was employed, Fig. 4.

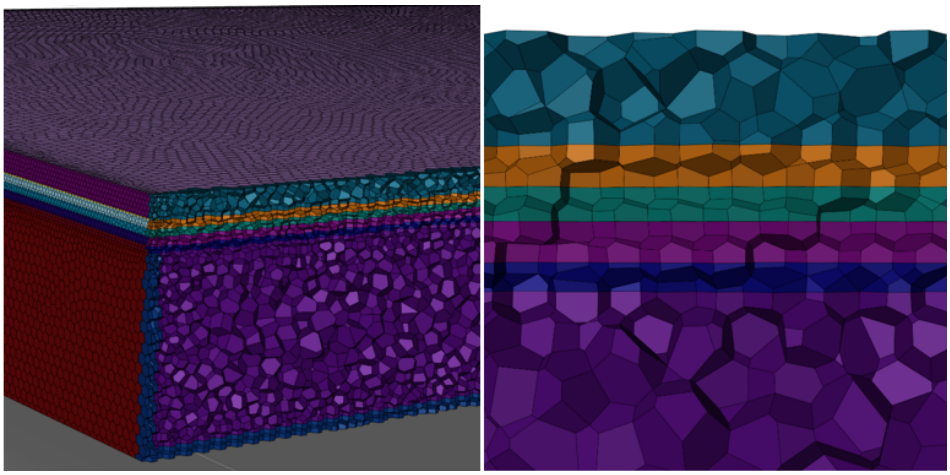

Fig. 4. The mesh used for numerical simulations (left), and mesh detail (right)

Polyhedral cells were chosen due to their ability to minimize numerical diffusion and promote faster convergence, which is particularly advantageous for complex geometries [23]. The mesh refinement was guided by the thickness of the thinnest layer (0.3 mm) to adequately resolve the geometry.

3. Experimental results and discussion

Hourly variations in wind speed and ambient temperature during the experimental period are shown in Fig. 5.

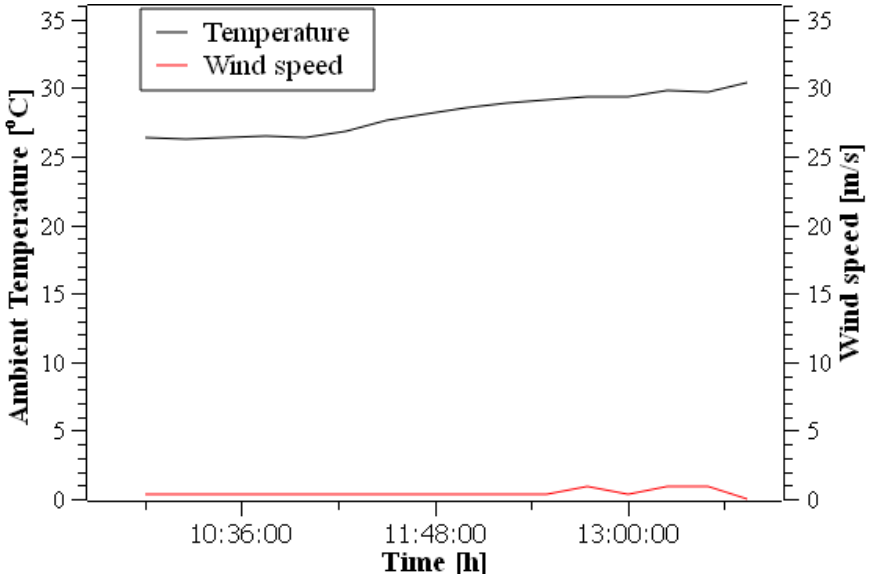

Fig. 5. Hourly variations in wind speed and ambient temperature during experiment.

The average measured ambient temperature was 28.1 °C, and the average wind speed was 0.47 m/s (Fig. 5). The ambient temperature through the experiment increased from 26.3 °C to 30.4 °C. The changes of the wind speed during the experiment were minimal, which allowed stable conditions for measuring and analyzing cooling effects. During the experiment, most of the day was cloudless. After 1:04 p.m., thinner clouds developed and partially blocked solar radiation, resulting in a change in the intensity of the solar radiation. During the experiment, solar radiation varied from 697 to 1047 W/m^2, at solar noon (12:36 p.m.) which corresponds to maximal ambient temperature of 29.3 °C, Fig. 6.

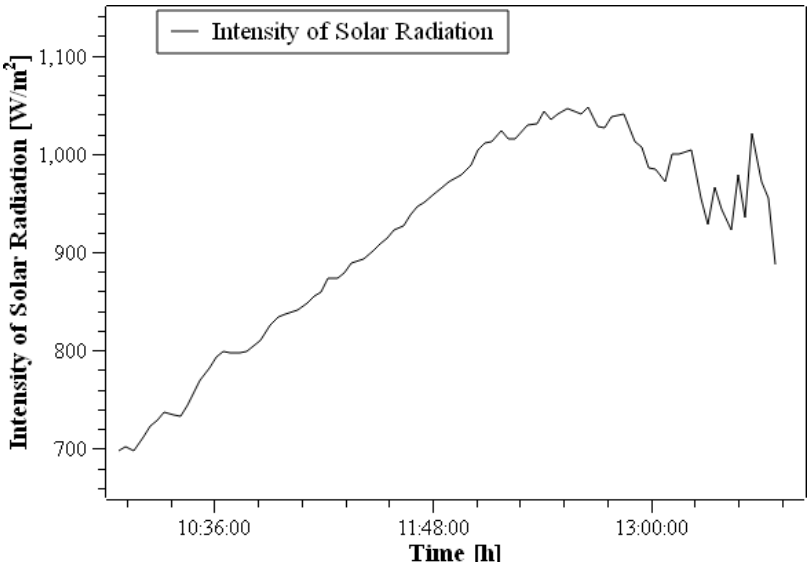

Fig. 6. The intensity of solar radiation during the experiment.

Similar observations of atmospheric conditions were noticed at the experimental site by the authors [11, 24, 25, 26].

In Fig. 7 and Fig. 8, the hourly variations in temperature of the front side of PV panel, and in power obtained from the PV system using water for cooling, are shown.

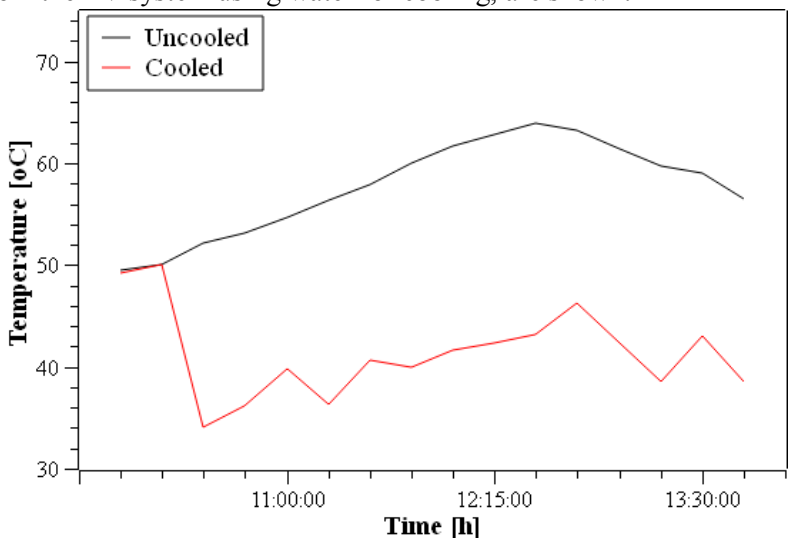

Fig. 7. The temperature of the front side of cooled and uncooled PV panel during the experiment.

Before the cooling process, at 10.15 a.m., the temperatures of cooled and uncooled panels were the same and amounted to 37.8 ^{o}C, Fig. 7. The values of the intensity of solar radiation and ambient temperature were 722 W/m^2 and 26.3 ^{o}C. The channel was empty before the process of cooling. At 10.15 a.m., filling of the channel on the back side of the panel started, thus the temperature of the panel started to decrease. During the experiment, the temperature of the front side of the PV panels was measured, more precisely, the temperature of PV panels front glass. After 25 minutes, from the beginning of the cooling, the reduction in the panel temperature was 22.1 ^{o}C, and the panel cooling rate was 1.18 ^{o}C/min.

At solar noon, the temperature of uncooled panel was 47.8 °C, of cooled panel it was 29.8 °C, and the ambient temperature was 29.3 °C. The temperature of uncooled and cooled panels at the end of experiment was 48 °C and 33.1 °C, respectively. At 1.29 p.m., the water circulation was stopped, and it was noticed that the temperature of the cooled and uncooled PV panel did not equalize even after 10 minutes. The results showed that the temperature of uncooled PV panel varies from 37.7 to 48 °C, with an average panel temperature of 43.6 °C, while the temperature of cooled panel varied from 16.7 to 37.8 °C during the experiment with the average temperature of 26.65 °C.

The maximum reduction in temperature of the front side of the panel was 23.1 °C at 11.13 p.m., with the ambient temperature of 26.8 °C. For comparison's sake, Menon *et al.* [11] have achieved a maximum temperature reduction of 15 °C at 12.00 p.m. while Sardarabadi *et al.* [27] reduced the PV module temperature by 11 °C.

During the experiment, alongside measuring the temperatures of the panels, the maximum power point, P_{mpp}, was recorded. Figure 8. illustrates the variation in P_{mpp} of the cooled and the uncooled panel during this process. Since the identical PV panels were used, the difference in P_{mpp} of the panels before cooling was minimally, about 0.1 W. There is an inverse proportion between the power output of the PV cell and the cell temperature.

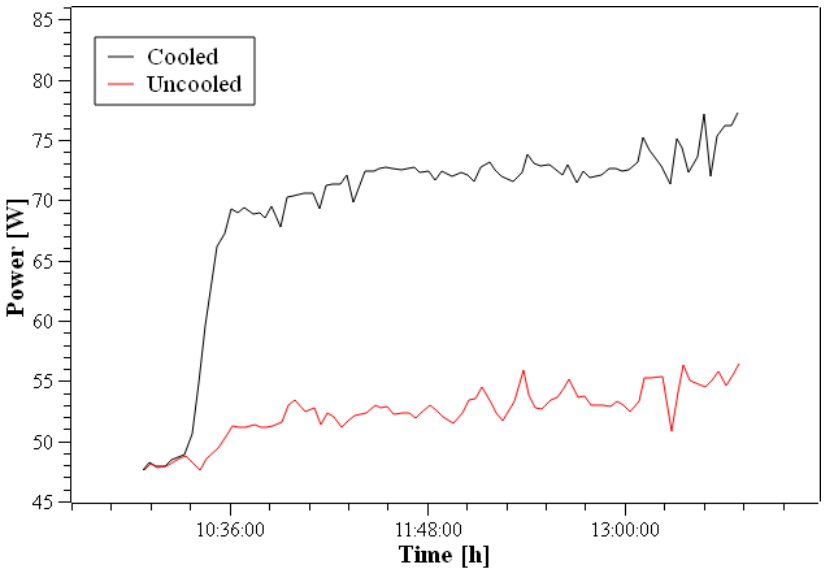

Fig. 8. The change of the maximum output power, P_{mpp}, for the cooled and uncooled panel, as a function of time.

After 15 minutes of cooling, the difference between power of cooled and uncooled panel was 16.76 W, which represent increase in power of 33.9 %. The average difference between the P_{mpp} was 16.77 W, which covers the energy consumption of the pump powering the water circulation system. This indicates that the cooling system is energy-efficient, with the energy gain exceeding the energy consumption, leading to a net increase in power production. At solar noon, the P_{mpp} of uncooled panel was 54.38 W, and of cooled panel it was 72.12 W, which represent increase in power of 32.6%. The low power of uncooled panel at solar noon, about half of its maximum power (100W), is a result of the panel being placed at the optimal fixed annual angle rather than the optimal angle for the month of June when the experiment was conducted. The development of cloudiness that happened at 1:04 p.m. also affects P_{mpp}, where the power change occurred and can be seen in Fig. 8. The maximum difference in power (22.74 W), was observed immediately before the end of the cooling at 1.29 p.m.

and corresponds to an increase in power of 41.75%. Similarly, Alzaabi *et al.* [28] improved the electrical power output by 15-20% with water-cooling from the back side. Yu *et al.* [29] increased electrical power by more than 15 % for a water-cooled PVT system. Nasrin *et al.* [30] focuses on enhancing the electrical power output of PVT systems, achieving an increase of approximately 9.2 % through the implementation of a water-cooling system. The PVT system performance achieved in this experimental study can be compared to the earlier studies by referring to Fig. 9.

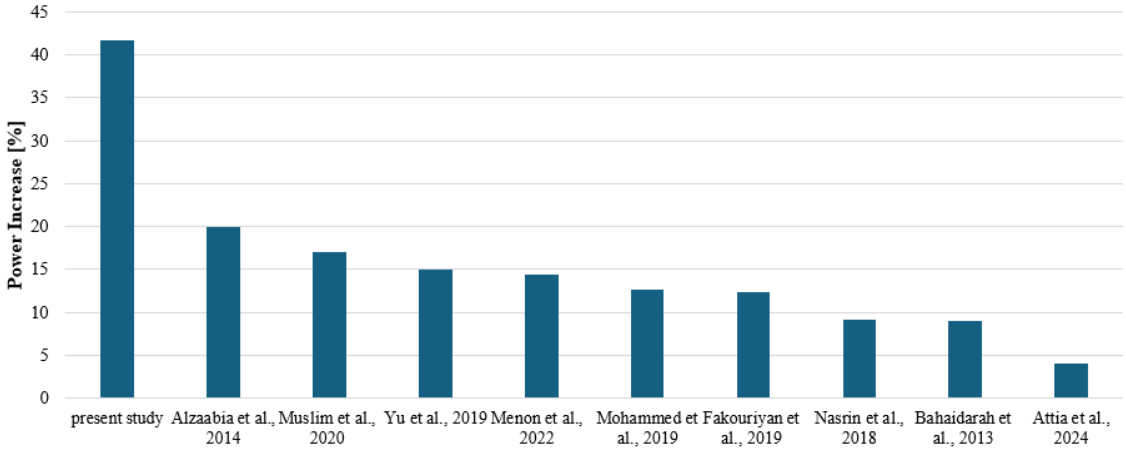

Fig. 9. The comparison between the current study and previously proposed designs for water-cooling from the back side.

Fig. 9 presents a comparison of various studies focused on increasing the efficiency of PV panels using water as a cooling fluid, from the back side. The current study reports the highest efficiency increase of 41.75%.

Figure 10. represents the I-V characteristic curves of cooled and uncooled PV panel, at the solar noon.

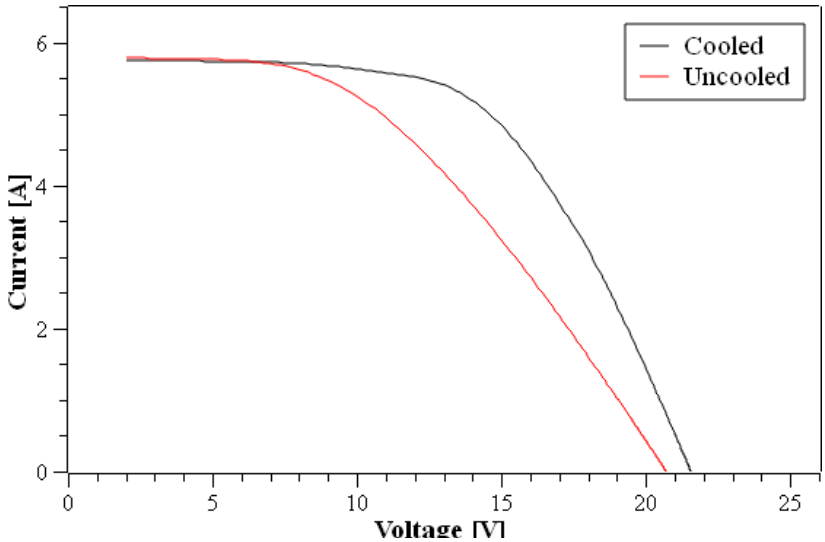

Fig. 10. I-V curve of cooled and uncooled PV panel, at the solar noon.

It can be seen from Fig. 10. that the I-V curve for the cooled panel is shifted to higher voltages. This shift is a result of the lower operating temperature, which positively affects the semiconductor material's performance within the solar cells. When the temperature of the PV panel decreases the V_{oc} increases. The V_{oc} of uncooled panel was 20.72 V, and of cooled panel was 21.55 V, at an ambient temperature of 29.1 °C. This represents a 5% increase in voltage.

This value indicates that the open circuit voltage increased to a value close to the STC value of PV panel, which amounts 21.6 V, although there is a significant difference between the operating temperature (29.1 °C) and the STC temperature (25 °C).

It should be noted that the I_{sc} of an uncooled and cooled PV panel was the same. The advantage of cooling the PV panel from the back is that it does not affect the I_{sc}, while cooling from the front has a negative effect [31]. Cooling from the front, the I_{sc} cooled panel has lower values than the uncooled one because, in the first situation, water participates in absorbing and dispersing part of the radiation, thereby reducing the intensity of the solar radiation reaching the solar panel.

Figure 11. represent the P-V characteristic curves of cooled and uncooled PV panel, at the solar noon and the change of the V_{mpp}, for the cooled and uncooled panel, as a function of time. The P-V curve typically peaks at a specific voltage, V_{mpp}, where the panel produces the P_{mpp}, under given conditions of sunlight intensity and temperature.

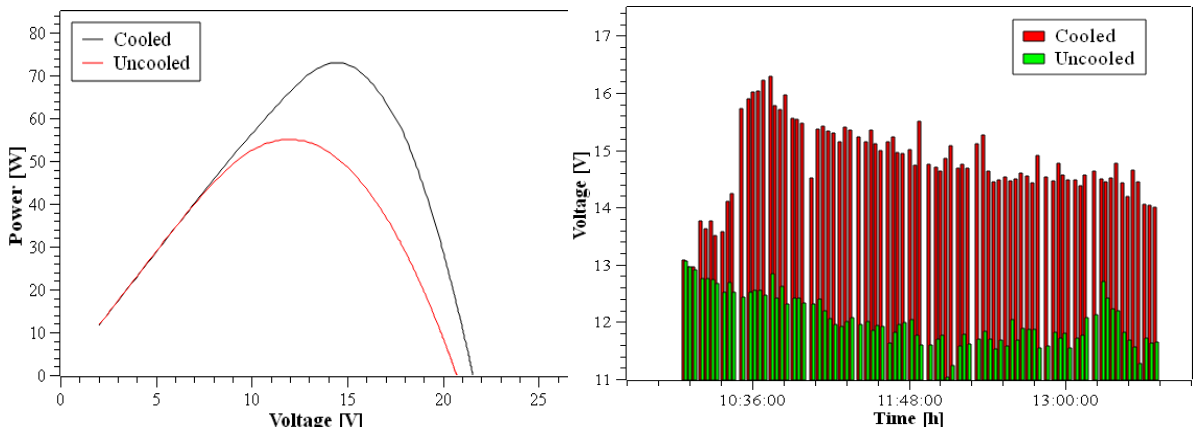

Fig. 11. P-V characteristic curves of PV panels, at the solar noon (left) and the change of the V_{mpp}, for the cooled and uncooled panel, as a function of time (right).

At a solar noon, the V_{mpp} which corresponds to the P_{mpp}, for cooled and uncooled PV panels are 14.60 V and 11.87 V, respectively. In this case, voltage increase is around 22.9%. The average difference between the V_{mpp} was 2.78 V.

Figures 12, 13, and 14 present a comparison of the thermal images of the actively cooled PV panel from both the experiment and the simulation. The temperature scale in the simulation was set to match the thermal image from the experiment to make it easier to notice the differences between the simulation and the experiment.

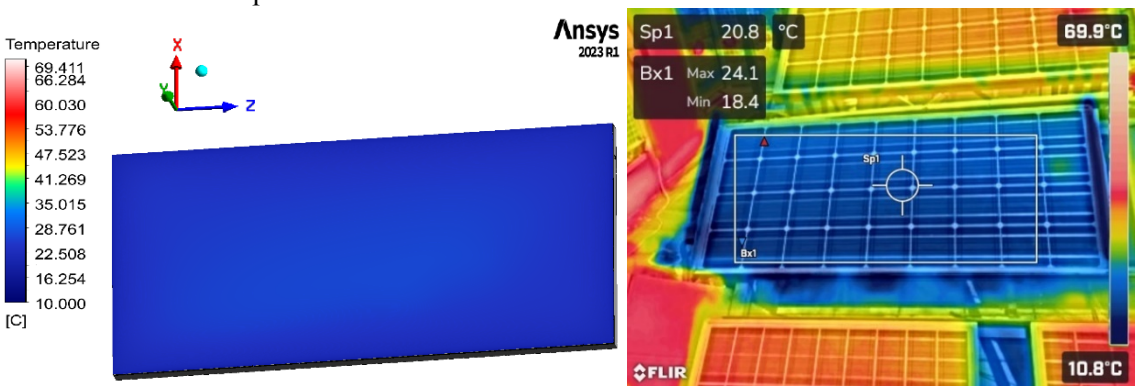

Fig. 12. Comparison of simulated (left) and experimental (right) thermal images of the PV panel at solar radiation of 854 W/m², at 11.08 a.m.

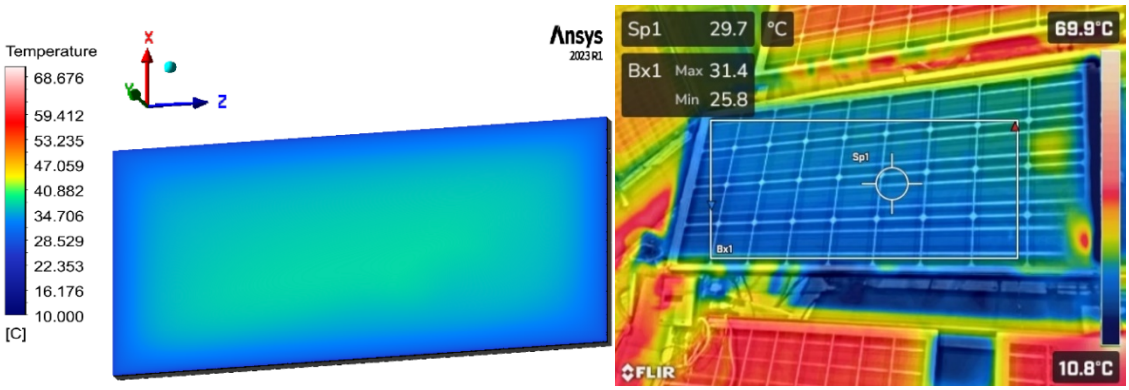

Fig. 13. Comparison of simulated (left) and experimental (right) thermal images of the PV panel at solar radiation of 1034 W/m², at 12.26 p.m.

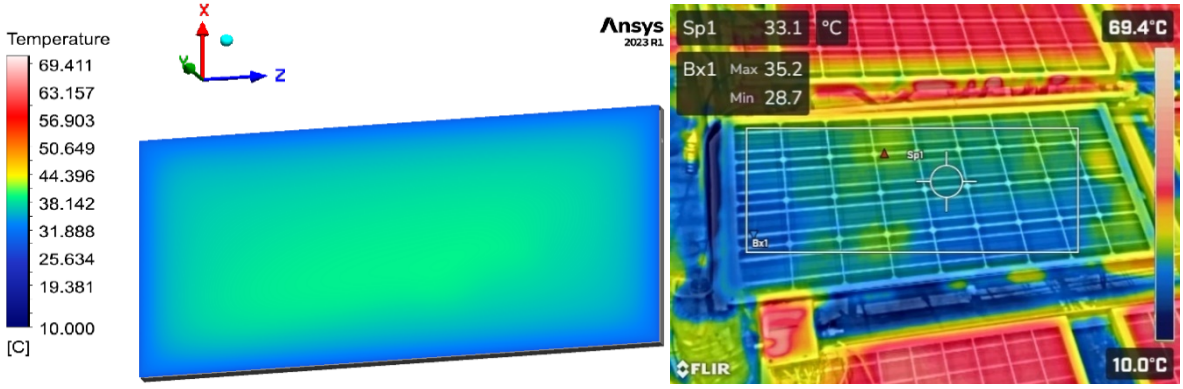

Fig. 14. Comparison of simulated (left) and experimental (right) thermal images of the PV panel at solar radiation of 979 W/m², at 1.29 p.m.

The comparison shows that the simulation provides accurate results, especially at solar radiation of 854, 979, and 1034 W/m². The thermal distributions observed in the simulation closely match those observed in the experiment, confirming that the simulation accurately reflects the thermal behavior of the PV panel under varying irradiance conditions. In the experimental thermal image of the PV panel, we can see that the area where the junction box is located has a higher temperature than the rest of the panel. The reason for that is because the area where is located junction box was not cooled. The junction box was not included in the simulation. For recently developed PV panels, the junction box has been significantly minimized with components integrated directly into the panel, allowing for better space utilization and improved thermal management. In Figure 12. we can see that the temperature of the PV panel from the simulation is almost uniform over the entire surface of the panel, while in the experiment it is seen that the bottom side of the panel has a lower panel temperature than the top. This is because the PV panel in the experiment is cooled from the bottom up and therefore the bottom part of the panel is slightly colder than the top. On Figures 13. and 14. of the simulation, it is evident that the temperature of the PV panel frame impacts the temperature distribution, whereas in the experiment, the influence of the frame temperature is negligible. The red area in the experimental thermal images of the PV panel in Figure 13. is a result of sunlight reflection from the panel's surface.

The temperatures obtained through both the experiment and simulation at various points on the PV panel are shown in Table 1. It was shown maximum, minimum and temperature of point in center of PV panel for the simulated and experimental thermal images of the PV panel. These points are given for 8 different solar radiation intensities.

Table 1. The temperatures obtained through both the experiment and simulation at various points on the PV panel.

		Experimetal results			Simulation results		
Time [h]	Solar Radiation [W/m^2]	T_{max}[°C]	T_{min}[°C]	T_{center}[°C]	T_{max}[°C]	T_{min}[°C]	T_{center}[°C]
10:40	799	19.0	14.2	16.7	19.9	14.8	17.1
11:08	854	24.1	18.4	20.8	23.9	18.5	21.2
11:13	872	27.7	17.7	23.2	27.1	17.2	24.2
11:19	878	26.8	22.6	25.4	26.1	22.1	25.9
11:52	971	28.4	21.4	26.1	28.6	22.1	27.2
12:06	1010	27.4	23.6	26.1	27.9	23.2	27.3
12:26	1034	31.4	25.8	29.7	31.3	25.5	30.5
1:29	979	35.2	28.7	33.1	35.8	28.5	34.7

Basen on the temperatures given in Table 1. the simulation agreement well with the experimental measurements of PV panel temperature, with maximum difference of about 1.6 °C. Small deviations between the experimental and simulated temperatures can be attributed to the area where the junction box is located. The temperature in this area of the PV panel was higher than in the rest of the panel.

The simulation results can be used to optimize parameters such as determining the optimal fluid flow through the cooling system, analyzing the temperature variations of the panels in different weather conditions, and optimizing the design of the cooling system, to achieve efficient and uniform cooling of the panels.

4. Conclusion

The performance of the PV panels drops significantly with an increase in the operating temperature. To solve the problem with overheating, the present work investigates the enhancement of PV panel's power using closed-loop system for active cooling of PV panel.

- The measurement results showed that the cooled panel achieved a minimum temperature of 16.7 °C, with an average panel temperature of 26.65 °C. The maximum reduction in temperature of the front side of the panel was 23.1 °C at 11.13 p.m., with the ambient temperature of 26.8 °C and solar radiation intensity of 872 W/m^2.
- At solar noon, the P_{mpp} of uncooled panel was 54.38 W, and of the cooled panel it was 72.12 W, which represents an increase in power of 32.6%. The average difference between the P_{mpp} was 16.77 W, which covers the energy consumption of the pump powering the water circulation system.
- The peak cooling effect was observed at 1:29 p.m., resulting in a 41.75% increase in power output.
- The V_{oc} of uncooled panel was 20.72 V, and the cooled panel was 21.55 V, at an ambient temperature of 29.1 °C. This represents a 5% increase in voltage.
- At solar noon, the V_{mpp} which corresponds to the P_{mpp}, for cooled and uncooled PV panels are 14.60 V and 11.87 V, respectively. In this case, voltage increase is around 22.9%.

- The simulation agrees well with the experimental measurements of PV panel temperature, with maximum difference of about 1.6 °C. Small deviations between the experimental and simulated temperatures can be attributed to the area where the junction box is located. The temperature in this area of the PV panel was higher than in the rest of the panel. The reason for that is because the area where the junction box is located was not cooled.

It can be stated that cooling the PV panels from the back side is a very effective method to reduce panel's temperature and increase efficiency. This system is ideal for use in an urban environment with individual prosumers, as advantages are the urban infrastructure, easy installation, extension of the operational life span of PV panels and increase of the PV electrical efficiency, which can result in more effective battery storage. The increased energy production can enhance the overall performance and energy yield of the system, which is crucial for maximizing the charging of the batteries. The simulation results can be used to optimize parameters such as determining the optimal fluid flow through the cooling system, analyzing the temperature variations of the panels in different weather conditions, and optimizing the design of the cooling system, to achieve efficient and uniform cooling of the panels. Additionally, the results provide valuable insights into the performance of the PVT system and enable forecasting of energy production under various climatic conditions.

Nomenclature

P_{mpp}- maximum power point, [W]
V_{oc}- open circuit voltage, [V]
I_{sc}- short circuit current, [A]
V_{mpp} – voltage which corresponds to the P_{mpp}, [V]

Acknowledgements

This research was done with the financial support of the Faculty of Sciences and Mathematics, University of Niš, Republic of Serbia, and of the Agreement 451-03-65/2024-03/200124 on the realization and financing of scientific research work of the Faculty of Sciences and Mathematics, University of Niš in 2023 by the Ministry of Education, Science and Technological Development of the Republic of Serbia. This research was financially supported by the Ministry of Science, Technological Development and Innovation of the Republic of Serbia (Contract No. 451-03-66/2024-03/200124).

This research was financially supported by the Ministry of Science, Technological Development and Innovation of the Republic of Serbia (Contract No. 451-03-66/2024-03).

References

[1] Al-Waeli, et al., An experimental investigation of SiC nanofluid as a base-fluid for a photovoltaic thermal PV/T system, *Energy Conversion and Management*, 142 (2017), pp. 547-558.

[2] Dwivedi, P., Advanced cooling techniques of PV modules: A state of art, *Case studies in thermal engineering*, 21 (2020), 100674.

[3] Muneeshwaran, M., et al., Performance improvement of photovoltaic modules via temperature homogeneity improvement, *Energy*, 203 (2020), 117816.

[4] Aboagye, B., et al., Investigation into the impacts of design, installation, operation and maintenance issues on performance and degradation of installed solar photovoltaic (PV) systems, *Energy for Sustainable Development*, 66 (2022), pp. 165-176.

[5] Moharram, K. A., et al., Enhancing the performance of photovoltaic panels by water cooling, *Ain Shams Engineering Journal*, 4(4) (2013), pp. 869-877.

[6] Al-Jamea, D. M. K., et al., Investigation on Water Immersing and Spraying for Cooling PV Panel, *International Review of Mechanical Engineering (I.RE.M.E.)*, 16 (2022).

[7] Kumar, R. S., et al., A Detailed Mathematical Modelling and Experimental Validation of Top Water Cooled Solar PV Module, *FME Transactions*, 47(3) (2019).

[8] Choi, S. U., Eastman, J. A., Enhancing thermal conductivity of fluids with nanoparticles (No. ANL/MSD/CP-84938; CONF-951135-29). Argonne National Lab.(ANL), Argonne, IL, United States, 1995.

[9] Prasher, R., et al., Thermal conductivity of nanoscale colloidal solutions (nanofluids), *Physical review letters*, 94(2) (2005), 025901.

[10] Elmir, M., et al., Numerical simulation of cooling a solar cell by forced convection in the presence of a nanofluid, *Energy Procedia*, 18 (2012), pp. 594-603.

[11] Menon, G. S., et al., Experimental investigations on unglazed photovoltaic-thermal (PVT) system using water and nanofluid cooling medium, *Renewable Energy*, 188 (2022), pp. 986-996.

[12] Rejeb, O., et al., Numerical and model validation of uncovered nanofluid sheet and tube type photovoltaic thermal solar system, *Energy Conversion and Management*, 110 (2016), pp. 367-377.

[13] Selmi, M., et al., Validation of CFD simulation for flat plate solar energy collector, *Renewable energy*, 33(3) (2008), pp. 383-387.

[14] Attia, M. E. H., et al., Design and performance optimization of a novel zigzag channeled solar photovoltaic thermal system: Numerical investigation and parametric analysis, *Journal of Cleaner Production*, 434 (2024), 140220.

[15] Khelifa, A., et al., Numerical analysis of the heat transfer and fluid flow of a novel water-based hybrid photovoltaic-thermal solar collector integrated with flax fibers as natural porous materials, *Renewable Energy*, 217 (2023), 119245.

[16] He, W., et al., Experimental study and performance analysis of a thermoelectric cooling and heating system driven by a photovoltaic/thermal system in summer and winter operation modes, *Energy conversion and management*, 84 (2014), pp. 41-49.

[17] Attia, M. E. H., et al., Numerical analysis and design of a novel solar photovoltaic thermal system using finned cooling channel structures embedded with air/TiO2–water nano bi-fluid, *Solar Energy*, 269 (2024), 112368.

[18] [18] Bahaidarah, H., et al., Performance evaluation of a PV (photovoltaic) module by back surface water cooling for hot climatic conditions, *Energy*, 59 (2013), pp. 445-453.

[19] Muslim, N. H., et al., Enhancement of solar photovoltaic module performance by using a water-cooling chamber for climatic conditions of Iraq, *International Journal of Renewable Energy Research (IJRER)*, 10(3) (2020), pp. 1103-1110.

[20] Fakouriyan, S., et al., Experimental analysis of a cooling system effect on photovoltaic panels' efficiency and its preheating water production, *Renewable Energy*, 134 (2019), pp. 1362-1368.

[21] Mohammed, F. M., et al., Performance enhancement of photovoltaic panel using Double-sides water glazing chambers cooling technique, *Al-Nahrain Journal for Engineering Sciences*, 22(1) (2019), pp. 22-30.

[22] Ansys Fluent User's Guide, ANSYS Inc, USA, Canonsburg, (2022).

[23] Balafas G. Polyhedral mesh generation for CFD-analysis of complex structures. Master Thesis. Tehnical University of Munich, Munich, (2014).

[24] Murali, S., et al., Design and performance evaluation of solar-LPG hybrid dryer for drying of shrimps, *Renewable Energy*, 147(2020), pp. 2417-2428.

[25] Murali, S., et al., Mathematical modeling of drying kinetics and quality characteristics of shrimps dried under a solar–LPG hybrid dryer, *Journal of Aquatic Food Product Technology*, 30(5) (2021), pp. 561-578.

[26] Murali, S., et al., Drying kinetics and quality characteristics of Indian mackerel (Rastrelliger kanagurta) in solar–electrical hybrid dryer, *Journal of Aquatic Food Product Technology*, 28(5) (2019), pp. 541-554.

[27] Sardarabadi, M., Passandideh-Fard, M., Experimental and numerical study of metal-oxides/water nanofluids as coolant in photovoltaic thermal systems (PVT), *Solar Energy Materials and Solar Cells*, 157(2016), pp. 533-542.

[28] Alzaabi, A. A., et al., Electrical/thermal performance of hybrid PV/T system in Sharjah, UAE. *International Journal of Smart Grid and Clean Energy*, 3(4) (2014), pp. 385-389.

[29] Yu, Y., et al., Testing and modelling an unglazed photovoltaic thermal collector for application in Sichuan Basin. *Applied Energy*, 242 (2019), pp. 931-941.

[30] Nasrin, R., et al., Water/MWCNT nanofluid based cooling system of PVT: Experimental and numerical research, *Renewable energy*, 121 (2018), pp. 286-300.

[31] Aste, N., et al., Performance monitoring and modeling of an uncovered photovoltaic-thermal (PVT) water collector. *Solar Energy*, 135 (2016), pp. 551-568.